Evaluation of SPMA and higher order sectorization for homogeneous SIR through macro sites

Evaluation of SPMA and Higher Order Sectorization for Homogeneous SIR through Macro Sites

Muhammad Usman Sheikh, Joonas Säe and Jukka Lempiäinen
Department of Electronics and Communications Engineering
Tampere University of Technology (TUT), Tampere, Finland
muhammad.sheikh@tut.fi, joonas.sae@tut.fi, jukka.lempiainen@tut.fi

***Abstract*—This paper highlights the performance of Single Path Multiple Access (SPMA) and discusses the performance comparison between higher order sectorization and SPMA in a macrocellular environment. The target of this paper is to emphasize the gains and significance of the novel concept of SPMA in achieving better and homogeneous SIR and enhanced system capacity in a macrocellular environment. This paper also explains the algorithm of SIR computation in SPMA. The results presented in this paper are based on sophisticated 3D ray tracing simulations performed with real world 3D building data and site locations from Seoul, South Korea. Macrocellular environment dominated with indoor users was considered for the research purpose of this paper. It is found that by increasing the order of sectorization, SIR along with spectral efficiency degrades due to the increase in inter-cell interference. However, as a result of better area spectral efficiency due to increased number of sectors (cells), the higher order sectorization offers more system capacity compared to the traditional 3-sector site. Furthermore, SPMA shows an outstanding performance and significantly improves the SIR for the individual user over the whole coverage area, and also remarkably increases the system capacity. In the environment under consideration, the simulation results reveal that SPMA can offer approximately 424 times more system capacity compared to the reference case of 3-sector site.**

Keywords—Macro cell; System Performance; High Order Sectorization; SPMA; 3D ray tracing; 5G

I. INTRODUCTION

In the modern society, every passing day the demand of high network capacity is rapidly increasing. Especially, in this era of advance mobile communications, people like to use their cellular phones everywhere in every situation. In the recent few years, the network technologies have evolved, so has the need for high data rates. The number of users using the internet and other applications with different quality of services is on ramp. Thus, in future systems, the operators are expecting to face severe problems in fulfilling the needs of their subscribers. One of the most difficult challenges, however, is to provide good services homogeneously over the whole cell area. Generally, a poor signal to interference ratio is due to the unwanted high interference coming from the neighboring cells. The most affected users are in the cell border areas, where the signal strength from the serving cell is not high enough, or the level of interference coming from the neighboring cells clearly dominates the serving cell [1].

The capacity in cell border areas is also a challenge for the operators. Traditionally, operators employ 3-sector sites with single 65° Half Power Beamwidth (HPBW) antenna in each sector to provide coverage and capacity in the network [1]. In hot spot areas with high capacity demand, a 6-sector site can be used to add more capacity to the system without adding an extra site or spectrum. In order to reduce the overlapping and to avoid the interference among the sectors in the case of higher order sectorization, an antenna with narrow HPBW is recommended e.g. 32° HPBW for 6-sector and 16° HPBW for a 12-sector site [21].

The innovative concept of SPMA proposed in [2] provides a possible way to communicate to every user through a needle beam of extremely low beamwidth. Instead of transmitting in wide area using a sectored antenna with wide HPBW, a highly directive beam is oriented to the user, minimizing the interference. The essence of the SPMA concept is based on the assumption that electrical metamaterials are used for antenna manufacturing and instead of using multipath transmission, the target is to utilize a single path to secure the link between the transmitter and receiver [2].

Higher order sectorization manages to add capacity in the system, but the problem of homogeneous grade of services over the whole cell area still exists. Mobile Stations (MSs) near the base station sites have strong signal strength and good quality of service or in other words good Signal to Interference plus Noise Ratio (SINR), thus high throughputs are possible at the nearby region of a base station. However, MSs near the cell border areas can experience poor coverage and bad SINR values, resulting in low throughputs. To improve this low throughput at cell border, several solutions are proposed in literature e.g., the use of Inter-Cell Interference Coordination (ICIC) [3-5], scheduling cell-edge users of different cells in different parts of the spectrum i.e. on different sub-carriers in order to avoid interference as included in 3GPP Release8 [6]. In the 3GPP Release 10, the ICIC method was improved and the enhanced Inter-Cell Interference Coordination (eICIC) scheme was introduced in [7], and then it was further improved in [8] by introducing the Further enhanced ICIC (FeICIC) feature. Although the general ICIC schemes are already included in the 3GPP specification to handle the interference, these methods may actually lower the network performance, because the nature of a load in the network is unevenly distributed and changes dynamically [3].

A different approach was introduced in the 3GPP Release 11 for Long Term Evolution Advanced (LTE-A), where Coordinated Multi Point Operation (CoMP) was introduced [9]. As the name suggests, CoMP can utilize several geographically separated Base Stations (BSs) to coordinate for transmitting and receiving from the users. Several CoMP related studies has been made in [10-12]. In order to work, as

with ICIC techniques, the CoMP also needs to have seamless cooperation between the neighboring BSs. The performance gain is closely related to Channel State Information (CSI) and depends on how well the CSI is delivered to the base station through a feedback channel.

Although both ICIC and CoMP methods are able to suppress the interference in the cell border areas, but the issue of not fully utilizing the whole system bandwidth remains there. At some occasions these techniques are able to use the whole system bandwidth, but only if the channel conditions between the different users in the same area are suitable for it. However, the SPMA exploits the spatial separation between the users, and serves each user with an independent individual beam, which allows the user to utilize whole available spectrum. By employing extremely narrow beams, SPMA manages to avoid interference to the neighbor users.

One of the aims of this paper is to highlight the problem of having a non-homogeneous distribution of SINR over the cell coverage area, and to propose a possible solution to overcome the issue of degraded quality of service for the users. This paper also shows the impact of higher order sectorization and SPMA on Signal to Interference Ratio (SIR) and on system capacity. In this paper, the SPMA concept is highlighted as a possible solution to improve the performance of mobile networks using existing macro sites, and it is proposed to make SPMA an integral part of Fifth Generation (5G) networks to meet the capacity requirement of future networks.

II. THEORY

A. 5G Cellular Networks

5G technology is yet not a standardized technology, but the research community has already started thinking and defining that how the next generation mobile network should look like. There are high expectations from 5G systems ranging from the supreme quality of experience to the support of wide range of applications with different quality of services. It is also expected that 5G will offer a few Gbps of throughput for individual user with 1000 times more system capacity compared to the Long Term Evolution System (LTE). The Fifth Generation of cellular networks will face the challenge of massive traffic volume, as it is forecasted that in the next ten years the mobile data volume per area will be increased by a thousandfold [13–15]. Another challenge will be high user data rates, which are also expected to increase ten to a hundred times the current throughputs [13–15]. The number of connected devices is also expected to rise in the coming years. Other challenges include the support of thousand times higher data volume, ten times longer battery life for low-power machine communication, and five times reduced end-to-end latency.

In order to achieve these objectives, different solutions are proposed in the literature [13–17]. One solution is the densification of sites, and concentrates on improving the small scale communications. For this kind of local area connections of this kind, the authors in [16] proposed a new radio interface called 5G flexible time division duplex (5GETLA). Other studies related to millimeter wave antenna propagation proposed the use of higher frequencies ranging from 30 GHz to 300 GHz [18–20] for communication in 5G cellular networks. These higher frequency ranges have large available bandwidth than the lower frequency bands (currently in use in cellular networks), but there are many other challenges for millimeter wave antenna propagation. Due to such a high frequency of operation, there is high pathloss which limits the signal propagation to a large distance. Millimeter wave propagation is basically meant for small cells and is not perfectly suitable for macrocellular environment. Generally, in macrocellular environment, an outdoor base station provides indoor coverage as well. However, due to large path losses it would be challenging to provide indoor coverage by using macro sites and millimeter wave communications.

B. Higher Order Sectorization

Generally, in cellular networks each outdoor base station has multiple sectors i.e. directional antennas are used instead of an omnidirectional antenna. In a conventional sectored site, each site has three sectors, where a directional 65° HPBW antenna with few dBs of antenna gain is used instead of an omnidirectional antenna. Higher order sectorization corresponds to the site with six or twelve sectors. Higher order sectorization at macrocellular level provides a solution to tackle the challenge of growing traffic demand, while reusing the existing macro site locations and spectrum in an efficient way. It is easy to upgrade from a traditional macro 3-sector site to a higher order sectored site, without involving complex technicalities and practicalities.

In [21], a performance comparison between 3-, 6- and 12-sector configuration was made to show the relative throughput gain offered by higher order sectorization compared a traditional 3-sector site. In [21], it was shown that compared to a traditional 3-sectored site, the 6-sectored and 12-sectored sites have clearly better throughputs e.g. with an Intersite Distance (ISD) of 1000m (the reference case), the relative throughput gain was 115.23% and 295.23% for the 6-sector and 12-sector site, respectively.

C. Shannon Capacity

Radio channel propagation conditions have a great effect on the performance of any wireless system. The upper bound, or widely known as the Shannon capacity, defines the maximum achievable capacity, C in bits/s, for a given channel [22]

$$C = W\langle \log_2\langle 1 + \Gamma \rangle \rangle, \quad (1)$$

where W is the bandwidth of the channel in Hz, radio channel condition is defined by SINR which is denoted by Γ, and $\langle \cdot \rangle$ denotes averaging. It should be noted that the SINR in (1) is in the linear scale. It can be seen from equation (1) that the system capacity is directly proportional to the system bandwidth i.e. higher the utilization of bandwidth higher will be the system capacity. Since the frequency spectrum is a scarce source, and cellular operators have only limited spectrum, therefore most of the time adding more spectrum is not a viable solution for operators to increase the system capacity. However, the second part of the equation (1) comprises of SINR, which can be improved by different techniques as also discussed in earlier sections.

To get a better comparison for different channel bandwidths, the Shannon bound is often divided with the used bandwidth W to get the average spectral efficiency ($\overline{\eta}$) in bits/s/Hz. It is defined as [23]

$$\overline{\eta} = \langle \log_2\langle 1 + \Gamma \rangle \rangle, \quad (2)$$

Average area spectral efficiency ($\overline{\eta}_{\text{area}}$) is defined as a product of average cell spectral density ($\overline{\eta}$) and the cell density (ρ_{cell}) as shown in equation (3) [23]

$$\overline{\eta}_{\text{area}}[\text{bits/s/Hz per km}^2] = \overline{\eta} \cdot \rho_{\text{cell}}. \quad (3)$$

The SIR at the j^{th} receiver point, Γ_j, can be calculated as given in equation (4), when imperfect orthogonality is assumed among the carriers (LTE) or code (UMTS) used for serving the users of the same cell [22]:

$$\Gamma_j = \frac{S_{j,\text{own}}}{I_{j,\text{own}} + \sum I_{j,\text{other}}}, \quad (4)$$

where S_j is the received signal power from the own serving cell at the j^{th} receiver point, $I_{j,\text{own}}$ and $I_{j,\text{other}}$ are the received interference power at the j^{th} receiver point coming from own cell and other cells, respectively.

D. Single Path Multiple Access (SPMA)

The key assumption behind the concept of Single Path Multiple Access (SPMA) is that new electrical materials are used in antenna manufacturing. These electrical materials include e.g. metamaterials [24, 25], graphene [26, 27], Carbon Nano Tube (CNT), Graphene Nano Ribbon (GNR) [30], and cloaking [31] etc. The main idea is to have a very narrow pencil-like needle beam dedicated to each user, such that each user served by an independent beam is re-using the frequency resources in each beam independently [2]. These radically narrow antenna beams are steered precisely to the user locations. In the traditional cellular theory, in case of a base station with wide sectors of 120° or 65° in macrocellular environment, the received power at RX is the sum of multipath components coming from TX. Whereas, in case of SPMA the beam intended for each user is assumed to be narrow enough such that the communication link between TX and RX is established with possibly only a single path, that is why it is known as Single Path Multiple Access. The concept of SPMA exploits the spatial characteristics of the radio channel. It can be said that SPMA is an evolved version of Space Division Multiple Access (SDMA). A centralized macro site approach is adopted by SPMA where a traditional base station with a finite number of sectors is replaced by a SPMA node. It will allow the reuse of a large number of existing macro site locations. A single SPMA node can have multiple needle beams with predefined beamwidth in an azimuth and elevation plane. A single SPMA node should be able to form multiple narrow beams at any particular time instant to serve multiple users at that particular time instant. It should be able to schedule different users in the time domain as well. The traditional concept of 'Cell' is no more valid for SPMA, as in the case of SPMA each user is assumed to have its own "Virtual Cell", where each user is re-using the frequency resources with a global reuse factor of one. Thus, in this case in the downlink direction every user is acting as an interferer to the other user, no matter whether the other user is served by own serving SPMA node or any other SPMA node [2].

In SPMA, the SIR at the m^{th} receiver point (Γ_m), is now calculated as follows:

$$\Gamma_m = \frac{S_m}{\sum I_{n,\text{own}} + \sum I_{p,\text{other}}}, n \neq m \; and \; p \neq m \quad (5)$$

where S_m is the received signal power at the m^{th} receiver point coming from the serving SPMA node intended for the m^{th} receiver point. $I_{n,\text{own}}$ is the received interference power at the m^{th} receiver point coming from the serving SPMA node intended for the n^{th} receiver point. Correspondingly, $I_{p,\text{other}}$ is the received interference power at the m^{th} receiver point coming from the other SPMA node intended for the p^{th} receiver point.

E. Ray Tracing

Traditionally, a nominal radio network plan is based on radio propagation models such as Okumura Hata, and COST231. These path loss models are used to estimate the maximum cell coverage based on link budget calculations. These propagation models are usually empirical or semi-empirical models, and are less complex, and are fast and easy to employ. Since these general models are based on measurement done in some other city, therefore they need fine tuning with respect to every new city before they are applied to get accurate results. Even after model tuning they are not able to model the signal propagation with high precision.

Ray tracing method provides an accurate way to model the signal propagation in actual radio environment. Ray tracing techniques, such as the Shoot and Bouncing Ray (SBR) and the Image Theory (IT) algorithm can be used to theoretically find all possible multipath components with a predefined number of reflections and diffractions between each Transmitter (TX) and Receiver (RX) points [28–30].

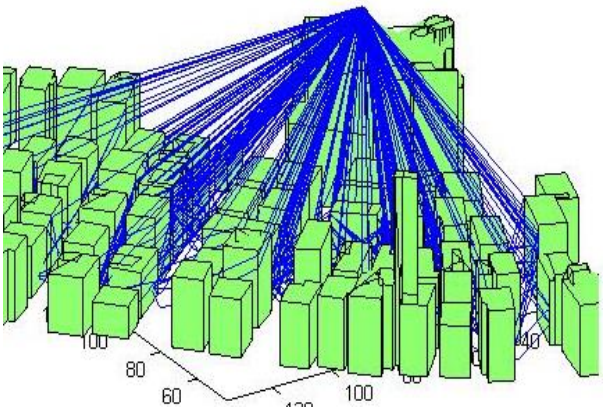

Fig. 1. 3D ray tracing in macro cellular environment.

Ray tracing simulations require three-dimensional (3D) model (map) of the environment to find the possible ray paths between TXs and RXs. For accurate modeling of the signal propagation in 3D environment, other than the detailed three dimensional map, the ray tracer requires additional minute information such as the ground and building material permittivity, building penetration loss, information about the

frequency of operation along with correct antenna heights and locations. Ray tracing is a complex and time consuming technique, but it helps in understanding the phenomena of signal propagation in a better way. Sophisticated 3D ray tracer used in [2] can even provide the information about the Direction of Departure (DoD) and Direction of Arrival (DoA) of a ray path in an azimuth plane, and the Angle of Departure (AoD) and Angle of Arrival (AoA) of ray path in an elevation plane. Fig. 1 shows an example of 3D ray tracing in macrocellular environment with antenna height above the roof top, and with finite number of reflections and diffractions using a 3D map.

III. Simulation Environment, Cases and Simulation Parameters

A. Simulation Tool and Simulation Environment

A massive campaign of simulations was done using a MATLAB as a simulation tool. Indigenous 3D ray tracing simulator based on Image Theory was developed in MATLAB. Unlike a quasi-three dimensional simulator the antenna height above the rooftops can be set in the used 3D ray tracer, which allows finding the signal path with diffraction from the rooftops. For the research work of this paper, unlike a hypothetical building grid environment i.e. regular Manhattan grid, or buildings with constant height and spacing, the real world environment was used. Actual practical network sites' locations and heights are used instead of regular hexagonal network layout, so that a fair comparison can be made between conventional 3-sector site, 6-sector site, and SPMA site. Around 1400m x 1400m area from South Korea is selected for the study purpose of this paper. The selected area with 3D building data using Google Earth can be seen in Fig. 2.

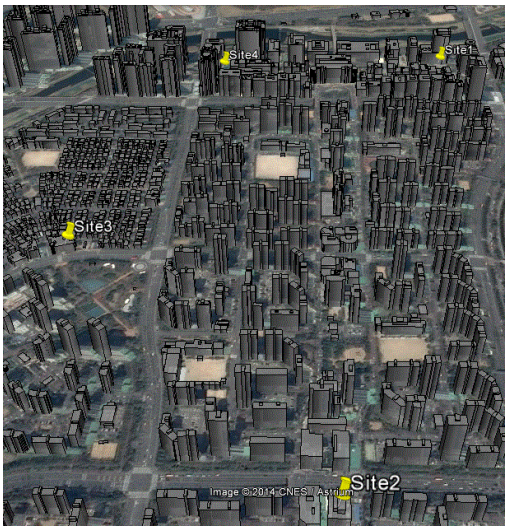

Fig. 2. Area under consideration from South Korea.

Selected area is covered by four sites. Site1, Site2, and Site3 are the rooftop sites, whereas Site4 is a wall mounted site with antennas for different sectors in different directions are mounted on the different walls of the building. The minimum intersite distance for all site location ranges from 625m to 750m, a typical value for a macrocellular site in an urban and dense urban area. There is urban area with low height buildings on the left side of the selected area and in the vicinity of Site3. The rest of the area can be categorized as dense urban area with high rise buildings. For the simulation purpose a total of 776 user locations were considered, out of which 95% of the users were considered in an indoor environment, and 5% of the users were considered in an outdoor environment. Irrespective of the population density and traffic profile, users' locations are randomly distributed over the area under consideration. For an indoor environment, users were placed on different floors depending upon the height of the building. Fig. 3 shows the location of the users in 2D map generated by MATLAB.

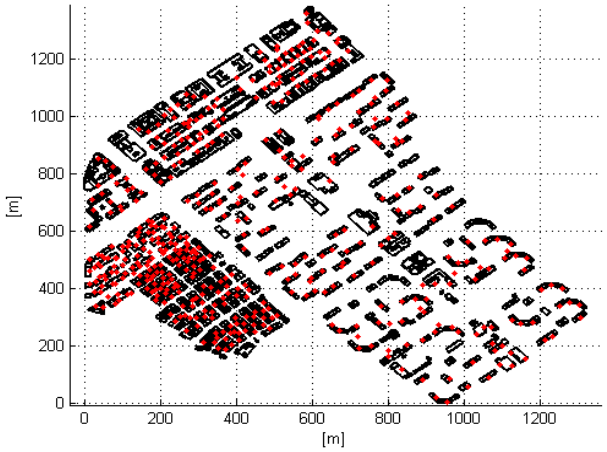

Fig. 3. User distribution.

B. SIR Computation for SPMA

In simulations, for the case of SPMA the process of computing SIR for each receiving point has four main stages, which are described as

i. Finding the strongest signal path for each user

3D ray tracing data acts as an input data for this stage. The simulator first determines the strongest signal path available for each user from all the SPMA nodes in a system, and then associates a user to the SPMA node (serving SPMA node) on the basis of the strongest signal path.

ii. Computing received power for each user with respect to the strongest signal path from the serving SPMA node

Each user is served by a needle beam in SPMA. The simulator computes the received power for each user location with respect to the horizontal and vertical HPBW of the SPMA beam. From 3D ray tracing data, all possible signal paths from the serving SPMA nodes are taken into account which lies within the horizontal and vertical HPBW of the respective SPMA beam.

iii. Computing interference coming from the serving SPMA node

At this stage, the simulator computes the interference coming from the "SERVING" SPMA node. In the SPMA system, every user served by a serving SPMA node also acts as an interferer as the same radio resources are reused in every SPMA beam. In Fig. 4, 'N' is the number of users served by a serving SPMA node.

iv. Computing interference coming from other SPMA nodes in the system

At this stage, the simulator computes the interference coming from the "OTHER" SPMA nodes. In Fig. 4, 'P' is the number of "OTHER" SPMA nodes (does not include the serving SPMA node) in the system, and 'Q' is the number of users served by each "OTHER" SPMA node. Finally, SIR is calculated by using the serving power, interference from the serving SPMA node and other SPMA nodes as shown in Fig. 4.

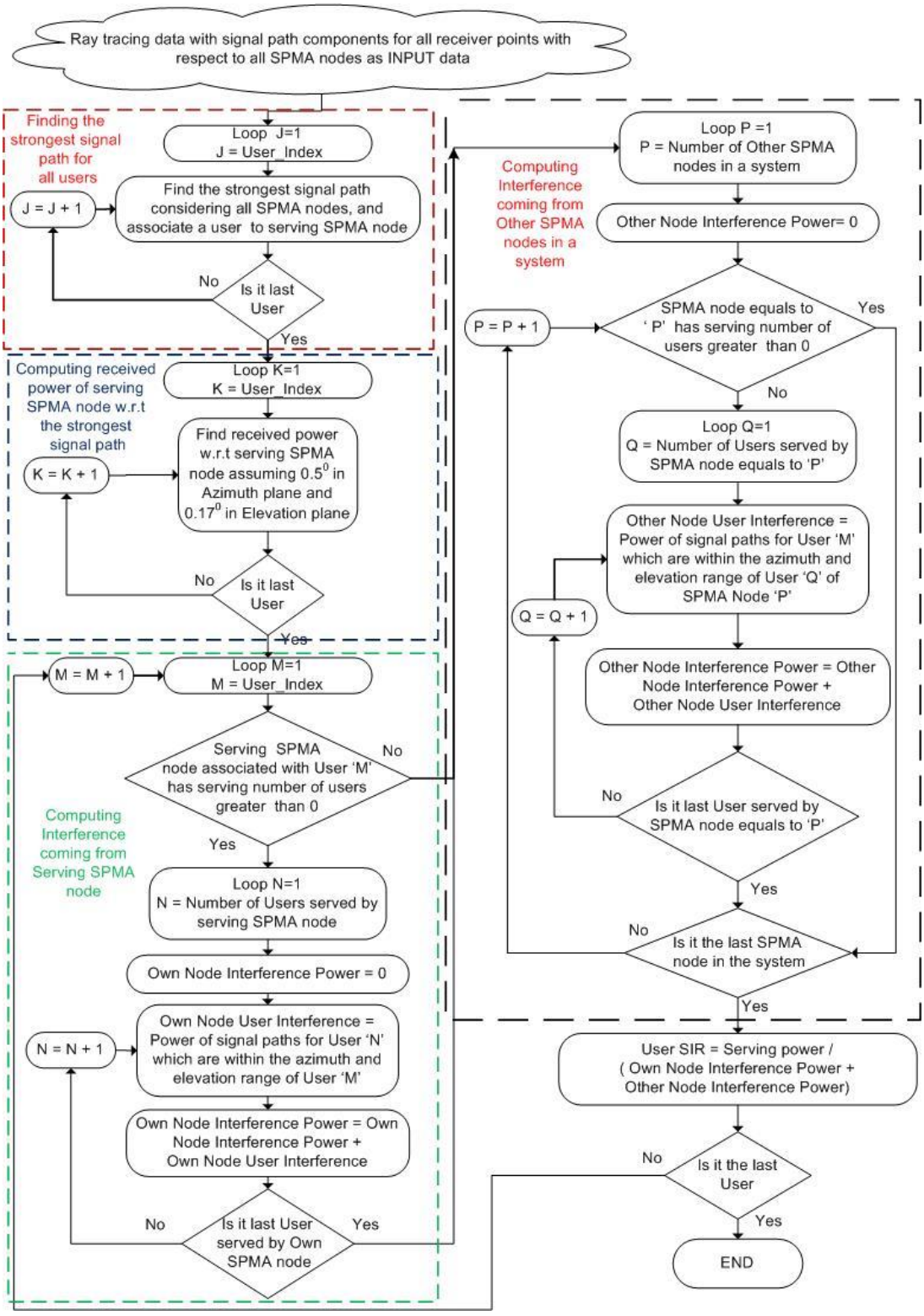

Fig. 4. Flow diagram of process for computing the SIR in SPMA system.

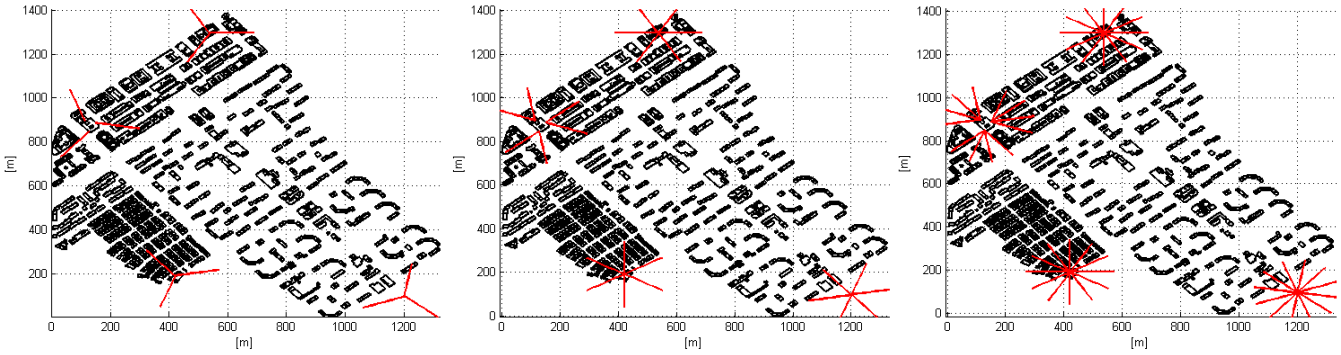

(a) (b) (c)

Fig. 5. Orientation of antennas for different simulation cases. a) 3-sector b) 6-sector and c) 12-sector.

C. *Simulation Cases and Simulation Parameters*

The simulation campaign for this paper consisted of four different cases.

- **3-sector site:** It is the conventional and traditional case in which each site has three sectors and every sector has single 65° HPBW antenna with no electrical or mechanical tilt, and with a maximum antenna gain of 15.39dB. For all the sites, there is a fix separation of 120° in an azimuth plane between the sectors of the same site. However, the base azimuth can be different for different sites as shown in Fig. 5a. This also acts as a reference case for comparing the results with other configurations.
- **6-sector site:** It is the case in which each site has six sectors, and every sector has single 32° HPBW antenna with no electrical or mechanical tilt, and with a maximum antenna gain of 18.20dB. For all the sites, there is a fix separation of 60° in an azimuth plane between the sectors of the same site. However, the base azimuth can be different for different sites as shown in Fig. 5b.
- **12-sector site:** In this case, each site comprises twelve narrow sectors, and every sector has single 16° HPBW antenna with no electrical or mechanical tilt, and with a maximum antenna gain of 21.15dB. For all the sites, there is a fix separation of 30° in an azimuth plane between the sectors of the same site. However, the base azimuth can be different for different sites as shown in Fig. 5c.
- **SPMA node:** In this last scenario, a SPMA node is assumed to create an extremely narrow needle beam for each serving individual user. No constraint was assumed on the number of serving users by single SPMA node. The needle beam is assumed to have 0.5° beamwidth in an azimuth plane and 0.17° in an elevation plane. The needle beam is assumed to have flat response with no additional gain in an azimuth and elevation plane. In this scenario, a needle beam is steered precisely to the serving user while keeping the user in the middle of the beam.

Other general simulation parameters are listed in Table I.

TABLE I. GENERAL SIMULATION PARAMETERS.

Parameter	Unit	Value
Operating frequency band	MHz	2600
Building penetration loss	dB	15
Ground permittivity		10
Building material permittivity		5
Outdoor user height	m	1.5
Indoor user height	m	Variable
Polarization		Vertical
Reflections	No.	2
Diffractions	No.	2
Rooftop diffraction		Enabled

IV. SIMULATION RESULTS AND ANALYSIS

Fig. 6a, Fig. 6b and Fig. 6c shows the SIR map for 3-sector, 6-sector and 12-sector case, respectively. It can be seen that for all three cases the best SIR values are achieved in the close vicinity of the site locations or in the regions with a possible LOS between the receiver point and site antenna. In the 3-sector site case there are also good samples of SIR in the middle left and the lower left corner (urban region) of the area under consideration. By watching the orientation of the antennas in Fig. 6a for 3-sector sites, it is evident that there is a clear dominant server and lack of interfering servers in the middle left region. The urban region mostly covered by Site3 also has better dominance area compared to the other sites. The SIR map shows that the most problematic region for the 3-sector case is lower middle and lower right portion of the simulated area due to the lack of a clear dominant server.

Orientation of the antennas in Fig. 6b for Site1 and Site4 clearly shows that the surrounding area is covered better with the 6-sector site case compared to the 3-sector site case, and this fact is also reflected in the results presented in Fig. 6b. In Fig. 6b, it can be seen that due to the addition of three more sectors compared to the 3-sector site case, SIR has improved the receiver points especially near Site1 and Site4, whereas slight degradation for few samples is also witnessed. SIR is also improved in the middle dense urban region, but SIR is affected badly in the urban region. In case of 12-sector site in Fig. 6c, SIR was degraded over the whole area due to overlapping of closely spaced sectors. Although narrow antennas of only 16° HPBW are used at 12-sector site, but still

there is high inter-cell interference coming from the other sectors of the same site.

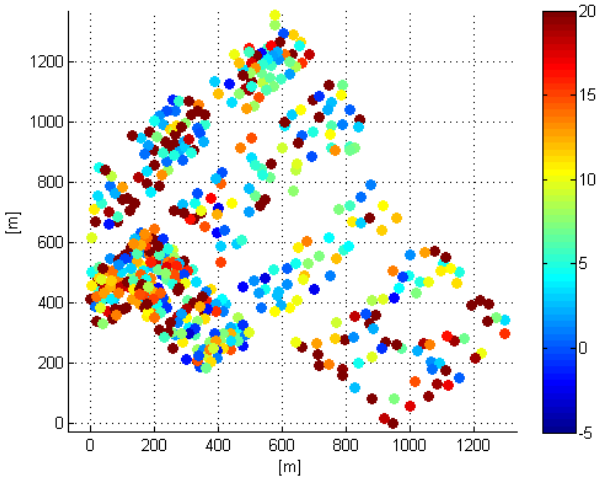

Fig. 6. (a) SIR map for 3-sector case.

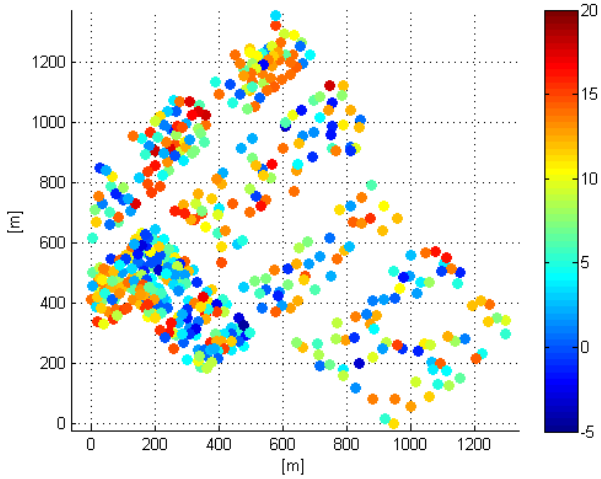

Fig. 6. (b) SIR map for 6-sector case.

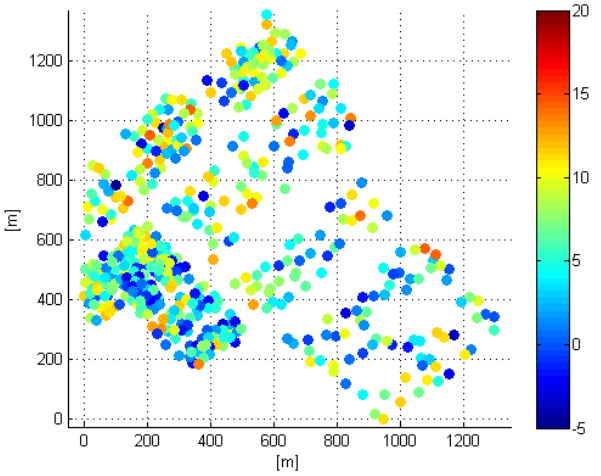

Fig. 6. (c) SIR map for 12-sector case.

The SIR map reveals that among the three cases discussed here, 3-sector site shows relatively better performance compared to 6-sector and 12-sector sites in terms of achieving better SIR. Hence, we can say that the achieved SIR is inversely proportional to the increasing order of sectorization, which means that by increasing the order of sectorization the SIR degrades. Fig. 7 shows the CDF plot of SIR achieved with 3-sector, 6-sector and 12-sector sites. More detail statistical analysis of the SIR results for different cases are presented later in Table III.

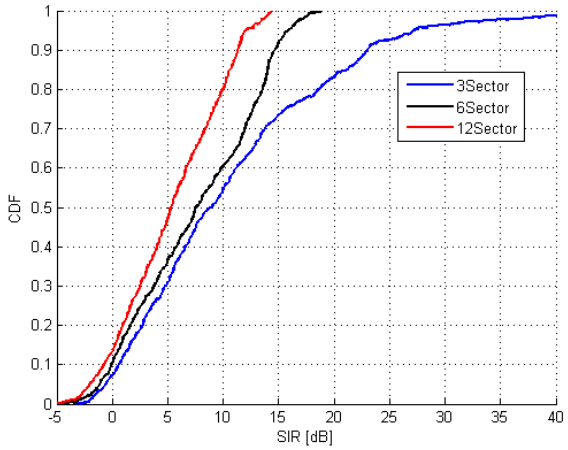

Fig. 7. CDF plot of SIR for 3-sector, 6-sector and 12-sector sites.

Overlapping zone (the number of servers) in the defined range of 'X' dB is used as a merit to establish the quality of the radio network plan. Like SIR, the overlapping zone is a network design Key Performance Indicator (KPI), which shows the caliber of the network plan from an interference point of view. The target of such criterion is to determine the dominance of the serving cell, and to learn about signal pollution. Existence of strong multiple servers at the same geographical location indicates high interference from other cells and it leads to the degradation of the system performance. Table II presents the results of the overlapping zone for 3-, 6- and 12-sector site cases.

TABLE II. RESULTS OF OVERLAPPING ZONE.

	3-sector [%]	**6-sector [%]**	**12-sector [%]**
Overlapping zone = 5dB			
Number of Server = 1	74.87	72.42	72.16
Number of Server = 2	20.23	20.75	20.88
Number of Server = 3	4.64	5.41	5.80
Number of Server ≥ 4	0.26	1.42	1.16
Overlapping zone = 7dB			
Number of Server = 1	65.21	63.79	60.70
Number of Server = 2	25.64	25.39	28.09
Number of Server = 3	7.35	7.99	7.86
Number of Server ≥ 4	1.80	2.83	3.55

There is slight difference in the results of the overlapping zone for 3-, 6- and 12-sector site cases, because the HPBW of antennas were selected with respect to the number and separation of sectors in an azimuth plane. Despite using narrow antennas for higher order sectorization, 3-sector sites provide better dominance area (No. of Servers = 1) compared to other two cases.

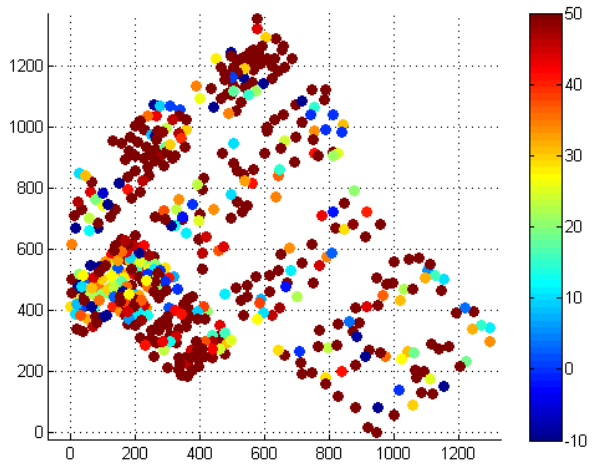

Fig. 8. SIR map for SPMA.

Fig. 8. shows the results of SIR for the special case of SPMA. For a better visualization of the results, the range of the color map is set from –10dB to 50dB. The results presented in Fig. 7 shows that SPMA outperforms other sectored antenna configurations. Simulation results validate the assumption made for SPMA that extremely directive narrow beams can help in avoiding the interference to the nearby users. Signal to interference ratio is enormously improved by the SPMA compared to the traditional sectored sites. High SIR is homogeneously achieved almost over the entire area under consideration, except few receiver points. However, at the same time a considerable number of users are found to have a low SIR of about -10dB. After deep analysis, it was found that when the distance between the users is too small then they experience low SIR with SPMA. It is worth mentioning here that for the results presented in Fig. 8, all 776 users were assumed to be active at that particular instant to compute SIR. Therefore, in SPMA a possible way to cope with such low SIR samples is to serve the nearby users in a different time domain.

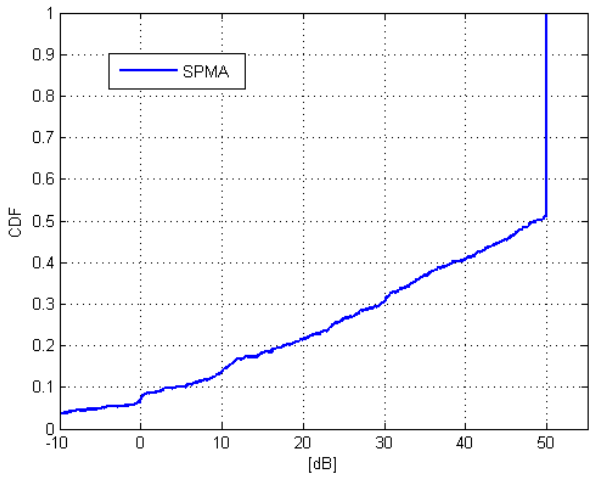

Fig. 9. CDF plot of SIR for SPMA.

In LTE there is OFDMA working over TDMA, in GSM there is FDMA over TDMA, which means resources are divided into the frequency domain and scheduling is done in the time domain. Similarly, here in the proposed concept of SPMA if two users are enough close to each other that the antenna is not able to distinguish them in a spatial domain, then they can be served in a different time domain. Time domain scheduling can still exist in SPMA along with spatial domain multiplexing. Therefore, the SIR results shown in Fig. 8 can be further improved by employing the time domain scheduling of the users.

Error! Reference source not found.. shows the CDF plot of SIR for the case of SPMA. In simulations, the maximum supported value of SIR was set to 50dB. In Fig. 8 the CDF curve shows that around 50% of the user locations, the achieved SIR was better or equal to 50dB.

Table III presents the comparative and statistical analysis of SIR for different cases considered in this paper. The obtained results present a very positive evaluation of the SPMA concept in achieving better SIR, since mean SIR of 35.78dB is achieved with SPMA which is far better than 10.8dB, 7.62dB, and 5.35dB attained by 3-, 6-, and 12-sector sites, respectively. Despite few very bad samples for SPMA, still the 10th percentile value of 4.28dB is the highest among all the configurations considered for the research work of this paper. The peak value of SIR gets considerably low due to increased overlapping among the sectors for higher order of sectorization.

TABLE III. COMPARATIVE STATISTICAL ANALYSIS OF SIR.

SIR	3-sector [dB]	6-sector [dB]	12-sector [dB]	SPMA [dB]
Mean	10.80	7.62	5.35	35.78
Median	8.92	7.54	5.28	48.77
Std	9.47	5.65	4.52	18.78
Minimum	–3.15	–4.42	–5.2	–10
Maximum	50.0	18.76	14.48	50
10th percentile	0.63	-0.04	–0.78	4.28
90th percentile	23.04	14.7	11.32	50

Table IV presents the capacity results. For a simulation campaign, four sites were considered for 3-, 6-, and 12-sector case. For post simulation capacity analysis, the cell density constitutes only those sectors which are facing towards the area under consideration. Therefore in Table IV, cell density is 8, 16, and 32 for 3-, 6-, and 12-sector case, respectively. In case of SPMA, each user is assumed to have its own virtual cell. SPMA considers a global reuse factor of one, which means the same frequency resources are being used by every user. Therefore, SPMA has a cell density of 776 virtual cells. The 10th percentile average spectral efficiency ($\bar{\eta}$) represents the average spectral efficiency of cell edge users or the users with bad coverage. SPMA not only offers higher area spectral efficiency ($\overline{\eta}_{\text{area}}$) due to large number of virtual cells, rather it also offers the highest average spectral efficiency among all other configurations. Mean spectral efficiency deteriorates with an increasing order of sectorization, but SPMA offers substantially high spectral efficiency compared to other cases by avoiding interference to the other users. Despite low spectral efficiency compared to a 3-sector site for higher order sectorization, the overall $\overline{\eta}_{area}$ improves by an increasing order of sectorization.

TABLE IV. CAPACITY RESULTS.

Cases	Cell Density	10 percentile $\overline{\eta}$ (bits/s/Hz)	10 percentile $\overline{\eta}_{area}$ (bits/s/Hz/km^2)	Mean $\overline{\eta}$ (bits/s/Hz)	Mean $\overline{\eta}_{area}$ (bps/Hz/ km^2)	Mean Capacity gain (times)
3-sector	8	1.11	8.88	3.70	29.62	1.0x
6-sector	16	0.99	15.89	2.76	44.16	1.49x
12-sector	32	0.87	28.04	2.15	68.80	2.32x
SPMA	776	1.88	1458	16.2	12571	424.42x

Thorough analysis of the simulation results showed that the system capacity gain starts to saturate by increasing the order of sectorization, and is not linear with an increasing order of sectorization. Ideally, moving from 3-sector to 6-sector should give two times, and moving from 3-sector to 12-sector should give four times the capacity gain. However, the simulation results revealed that in the considered scenario the 6-sector and 12-sector site offers only 1.49 and 2.32 times more system capacity compared to the reference 3-sector site case, respectively. Furthermore, SPMA provides a gigantic increase in system capacity and offers 424.42 times more system capacity compared to the traditional 3-sector site. This mammoth increase in system capacity by SPMA would help in achieving the high capacity requirement in 5G cellular networks.

V. CONCLUSIONS

In this article, we investigated the performance of higher order sectorization and single path multiple access in a real world macrocellular environment dominated by indoor users by performing 3D ray tracing simulations. A comprehensive comparative system level performance analysis was carried out between the traditional 3-sector site, higher order sectorization, and SPMA. Post simulations analysis revealed that the 3-sector site shows better performance in achieving better SIR compared to the other higher order sectorization cases. Mean SIR deteriorates by approximately 2.18dB and 4.45dB in 6-sector and 12-sector cases, respectively, compared to a 3-sector site case. It was found that higher order sectorization reduces the spectral efficiency due to high interference from neighbor cells, but the overall system capacity increases due to an increase in number of serving cells. It was also observed that the over lapping zones between the cells can be controlled by employing narrow beamwidth antennas for higher order sectorization. Higher order sectorization enhanced the system capacity, but the improvement in the system capacity by 6- and 12-sector sites was limited to 1.49 and 2.32 times, respectively, compared to the reference 3-sector site case. Therefore, the capacity requirement for 5G can't be met with higher order sectorization only.

In this paper, the significance of SPMA in achieving high SIR over the whole coverage area and a huge increase in the system capacity is shown. Results presented in this paper showed that by keeping the horizontal HPBW of 0.5° and vertical HPBW of 0.17°, an enormous increase in the system capacity can be achieved by using SPMA in macrocellular environment. SPMA not only improves the area spectral efficiency due to a large number of virtual cells, rather it also improves the spectral efficiency by avoiding unnecessary interference to the other users due to extremely narrow beams. In the simulation scenario considered for the research purpose of this paper, SPMA offered 424.42 times more system capacity compared to a 3-sector site, without adding extra spectrum or using multi-stream transmission. Thus, the results presented in this paper show the potential significance of the SPMA concept, that it can provide a multifold increase in the capacity of a centralized macro site. Other advantages of SPMA are the reusability of existing macro sites and low operational cost. These results show that SPMA can be considered as an alternate solution to achieve the target of thousand times more capacity compared to LTE for fifth generation cellular networks.

Although, yet the scientific community is not able to device such an antenna as proposed in this paper. However, considering the references provided in the paper, it is strongly believed that it is not far in future when a breakthrough in material technology will make it possible to have such an advanced antenna. The results presented in the paper are with respect to the environment under consideration and assuming static users. The performance of SPMA cannot be generalized on the basis of given results, as it depends on many factors like site type (macro, micro, pico), area type (Dense Urban, Urban, Rural), etc. The concept of SPMA is still in the developing phase, therefore issues like mobility, beam tracking overheads, computational complexity and energy efficiency needs to be addressed

For the future work, it would be interesting to investigate that how the SPMA gain is affected by increasing the HPBW of narrow SPMA beams, as SPMA is a highly interference sensitive system.

ACKNOWLEDGMENT

Authors would like to thank European Communications Engineering (ECE) Ltd and European Celtic-Plus project SHARING for supporting this research work.

.

REFERENCES

[1] J. Itkonen, B. Tuzson, J. Lempiäinen, "Assessment of Network Layouts for CDMA Radio Access," in EURASIP Journal on Wireless Communications and Networking, Volume 2008 (2008).

[2] M.U. Sheikh, J. Lempiäinen, "Will New Antenna Material enable Single Path Multiple Access (SPMA)? In Springer Journal on Wireless Personal Communications, Volume 78, Issue 2(2014) September, Page 979-994.

[3] A. Hamza, S.S. Khalifa, H.S. Hamza and K. Elsayed, "'A Survey on Inter-Cell Interference Coordination Techniques in OFDMA-Based Cellular Networks," Communications Surveys & Tutorials, IEEE, vol. 15, no. 4, pp. 1642-1670.

[4] C. Kosta, B. Hunt, A. Quddus and R. Tafazolli, "'On Interference Avoidance Through Inter-Cell Interference Coordination (ICIC) Based on OFDMA Mobile Systems," Communications Surveys & Tutorials, IEEE, vol. 15, no. 3, pp. 973-995.

[5] C.G. Gerlach, I. Karla, A. Weber, L. Ewe, H. Bakker, E. Kuehn and A. Rao, "'ICIC in DL and UL with network distributed and self-organized resource assignment algorithms in LTE," Bell Labs Technical Journal, vol. 15, no. 3, pp. 43-62.

[6] 3GPP, E-UTRA and E-UTRAN Overall description: Stage 2 (Release 8), 3GPP TS 36.300 V8.0.0, Apr. 2007. Available (Sep. 2014): http://www.3gpp.org.

[7] 3GPP, E-UTRA and E-UTRAN Overall description: Stage 2 (Release 10), 3GPP TS 36.300 V10.2.0, Dec. 2010. Available (Sep. 2014): http://www.3gpp.org.

[8] 3GPP, E-UTRA and E-UTRAN Overall description: Stage 2 (Release 10), 3GPP TS 36.300 V11.3.0, Dec. 2012. Available (Sep. 2014): http://www.3gpp.org.

[9] 3GPP, "Evolved Universal terrestrial radio access (E-UTRA) and evolved universal terrestrial radio access network (E-UTRAN); co-ordinated multi-point operation for LTE physical layer aspects (Release 11)," 3GPP TR 36.819 V11.2.0, Sept. 2013. Available (Sep. 2014): http://www.3gpp.org.

[10] Shaohui Sun, Qiubin Gao, Ying Peng, Yingmin Wang and Lingyang Song, "'Interference management through CoMP in 3GPP LTE-advanced networks," Wireless Communications, IEEE, vol. 20, no. 1, pp. 59-66.

[11] Chenyang Yang, Shengqian Han, Xueying Hou and A. Molisch, "'How do we design CoMP to achieve its promised potential?" Wireless Communications, IEEE, vol. 20, no. 1, pp. 67-74.

[12] Q. Cui, H. Wang, P. Hu, X. Tao, P. Zhang, J. Hamalainen and L. Xia, "'Evolution of Limited-Feedback CoMP Systems from 4G to 5G: CoMP Features and Limited-Feedback Approaches," Vehicular Technology Magazine, IEEE, vol. 9, no. 3, pp. 94-103.

[13] A. Osseiran, V. Braun, T. Hidekazu, P. Marsch, H. Schotten, H. Tullberg, M.A. Uusitalo, M. Schellman, " The Foundation of the Mobile and Wireless Communications System for 2020 and Beyond: Challenges, Enablers and Technology Solutions" in *Proceedings of 77th IEEE Vehicular Technology Conference (VTC Spring)*, Dresden, June 2013, pp. 1–5.

[14] J.G. Andrews, S. Buzzi, Wan Choi, S.V. Hanly, A. Lozano, A.K. Soong and J.C. Zhang, "'What Will 5G Be?" Selected Areas in Communications, IEEE Journal on, vol. 32, no. 6, pp. 1065-1082.

[15] A. Osseiran, F. Boccardi, V. Braun, K. Kusume, P. Marsch, M. Maternia, O. Queseth, M. Schellmann, H. Schotten, H. Taoka, H. Tullberg, M.A. Uusitalo, B. Timus and M. Fallgren, "'Scenarios for 5G mobile and wireless communications: the vision of the METIS project," Communications Magazine, IEEE, vol. 52, no. 5, pp. 26-35.

[16] T.A. Levanen, J. Pirskanen, T. Koskela, J. Talvitie and M. Valkama, "Radio Interface Evolution Towards 5G and Enhanced Local Area Communications," Access, IEEE, vol. 2, pp. 1005-1029.

[17] E. Hossain, M. Rasti, H. Tabassum and A. Abdelnasser, "'Evolution toward 5G multi-tier cellular wireless networks: An interference management perspective," Wireless Communications, IEEE, vol. 21, no. 3, pp. 118-127.

[18] T.S. Rappaport, Shu Sun, R. Mayzus, Hang Zhao, Y. Azar, K. Wang, G.N. Wong, J.K. Schulz, M. Samimi and F. Gutierrez, "'Millimeter Wave Mobile Communications for 5G Cellular: It Will Work!" Access, IEEE, vol. 1, pp. 335-349.

[19] J. Karjalainen, M. Nekovee, H. Benn, W. Kim, J. Park and H. Sungsoo, "'Challenges and opportunities of mm-wave communication in 5G networks," Cognitive Radio Oriented Wireless Networks and Communications (CROWNCOM), 2014 9th International Conference on, pp. 372-376.

[20] A. Ghosh, T.A. Thomas, M.C. Cudak, R. Ratasuk, P. Moorut, F.W. Vook, T.S. Rappaport, G.R. Maccartney, Shu Sun and Shuai Nie, "'Millimeter-Wave Enhanced Local Area Systems: A High-Data-Rate Approach for Future Wireless Networks," Selected Areas in Communications, IEEE Journal on, vol. 32, no. 6, pp. 1152-1163.

[21] M.U. Sheikh, and J. Lempiäinen., "Advanced Antenna Techniques and Higher Order Sectorization with Novel Network Tessellation for Enhancing Macro Cell Capacity in DC-HSDPA Network", International Journal of Wireless & Mobile Networks. Vol. 5, No.5, October 2013.

[22] C. Shannon, "Communication in the presence of noise," Proceedings of the IRE, vol. 37, no. 1, pp. 10–21, Jan 1949.

[23] S.F. Yunas, M. Valkama, J. Niemelä, "Spectral Efficiency of Dynamic DAS with Extreme Down-tilt Antenna Configuration" in The 7th International WDN Workshop on Cooperative and Heterogeneous Cellular Networks (WDN-CN2014), Washington D.C., September 2014, pp. 1–7.

[24] F. Zhu, Q. Lin, J. Hu, "A directive patch antenna with a metamaterial cover," Microwave Conference Proceedings, 2005. APMC 2005. Asia-Pacific Conference Proceedings, vol.3, no., pp. 3 pp., 4-7 Dec. 2005.

[25] H. Jun, Y. Chun-seng, L. Qing-chun, "A new patch antenna with meta material cover", Journal of Zhejiang University Science A, 2005. Doi:10.1631/jzus.2006.A0089.

[26] J. S. Gomez-Diaz, J. Perruisseau-Carrier, "Microwave to THz properties of graphene and potential antenna applications," International Symposium on Antennas and Propagation (ISAP), 2012, pp.239-242, Oct. 29 2012-Nov. 2 2012 .

[27] I. Llatser, C. Kremers, D.N. Chigrin, J.M. Jornet, M.C. Lemme, A. Cabellos-Aparicio, and E. Alarcon, "Characterization of graphene-based nano-antennas in the terahertz band," 6th European Conference on Antennas and Propagation (EUCAP), 2012, pp.194-198, 26-30 March 2012.

[28] H.W. Son, and N.H. Myung, "A deterministic ray tube method for microcellular wave propagation prediction model," Antennas and Propagation, IEEE Transactions , vol.47, no.8, pp.1344-1350, Aug 1999.

[29] D.N. Schettino, F.J.S. Moreira, C.G. Rego, "Efficient Ray Tracing for Radio Channel Characterization of Urban Scenarios," Magnetics, IEEE Transactions on , vol.43, no.4, pp.1305-1308, April 2007

[30] S. Soni and A. Bhattacharya, "An efficient two-dimensional ray-tracing algorithm", International Journal of Electronics and Communication (AEU), volume 66, issue 6, pp. 439-447, June 2012.

[31] Graphene-Based Nano-Antennas for Electromagnetic Nano communications in the Terahertz Band," In Proc. of 4th European Conference on Antennas and Propagation, EUCAP, April 2010.

[32] Schurig. D., et al. "Metamaterial Electromagnetic Cloak at Microwave Frequencies". Science, vol. 314, pp: 977–980. Novemeber, 2006. DOI: 10.1126/science.1133628